Integrative and Comparative Biology Advance Access published September 21, 2011
Integrative and Comparative Biology, pp. 1–17
doi:10.1093/icb/icr112

SYMPOSIUM

Using Physical Models to Study the Gliding Performance of Extinct Animals

M. A. R. Koehl,[1] Dennis Evangelista and Karen Yang

Department of Integrative Biology, University of California Berkeley, CA 94720-3140, USA

From the symposium "The Biomechanics and Behavior of Gliding Flight" presented at the annual meeting of the Society for Integrative and Comparative Biology, January 3–7, 2011, at Salt Lake City, Utah.

[1]E-mail: cnidaria@berkeley.edu

Synopsis Aerodynamic studies using physical models of fossil organisms can provide quantitative information about how performance of defined activities, such as gliding, depends on specific morphological features. Such analyses allow us to rule out hypotheses about the function of extinct organisms that are not physically plausible and to determine if and how specific morphological features and postures affect performance. The purpose of this article is to provide a practical guide for the design of dynamically scaled physical models to study the gliding of extinct animals using examples from our research on the theropod dinosaur, †*Microraptor gui*, which had flight feathers on its hind limbs as well as on its forelimbs. Analysis of the aerodynamics of †*M. gui* can shed light on the design of gliders with large surfaces posterior to the center of mass and provide functional information to evolutionary biologists trying to unravel the origins of flight in the dinosaurian ancestors and sister groups to birds. Measurements of lift, drag, side force, and moments in pitch, roll, and yaw on models in a wind tunnel can be used to calculate indices of gliding and parachuting performance, aerodynamic static stability, and control effectiveness in maneuvering. These indices permit the aerodynamic performance of bodies of different shape, size, stiffness, texture, and posture to be compared and thus can provide insights about the design of gliders, both biological and man-made. Our measurements of maximum lift-to-drag ratios of 2.5–3.1 for physical models of †*M. gui* suggest that its gliding performance was similar to that of flying squirrels and that the various leg postures that might have been used by †*M. gui* make little difference to that aspect of aerodynamic performance. We found that body orientation relative to the movement of air past the animal determines whether it is difficult or easy to maneuver.

Introduction

Many lines of evidence are used to form inferences and test hypotheses about how extinct organisms functioned. These in turn are used to suggest selective factors that might have been important in their evolution or to propose ecological interactions in paleocommunities. For mechanical functions such as locomotion, biomechanical analysis of fossil organisms can provide quantitative information about how performance of defined activities depends on specific morphological features. Such analyses allow us to rule out hypotheses about the function of extinct organisms that are not physically plausible and to determine if and how specific morphological features affect performance. Many examples of using biomechanics to aid in interpretation of the attributes of fossil organisms are reviewed by Rayner and Wootton (1991) and Hutchenson and Allen (2009).

Usefulness of models

Models, both physical and mathematical, can be powerful tools for exploring the mechanical performance of living and extinct organisms. By varying specific morphological features or kinematic parameters in such models, the effects of these structures and behaviors on defined functions performed by the organisms can be quantified. Working with models, rather than with living organisms, allows the performance consequences of specific changes in defined parameters to be determined while holding other

parameters constant (e.g., Koehl 2003; Hutchenson and Allen 2009) and also permits the interactions between different features to be assessed in a systematic way (Emerson et al. 1990). For example, mathematical models of the fluid mechanics of jet propulsion by cnidarian medusae explored how body shape and swimming kinematics affect the size at which the ratio of efficiency to cost of locomotion is maximized (Daniel 1983) and revealed how the interactions between jellyfish and the water constrain the morphological diversity of lineages of these animals (Dabiri et al. 2007). Similarly, a computer simulation of running by theropod dinosaurs that systematically varied maximal velocity of muscle contraction and mass of limb muscle revealed the parameter space in which one or the other of these factors limits running speed (Sellers and Manning 2007). Physical models were used to measure the consequences of shape, flexural stiffness, surface texture, and orientation on the hydrodynamic forces experienced by sea anemones exposed to ambient water currents (Koehl 1977). Likewise, the effects of enlarged hands and feet, skin flaps, body shape, and limb posture on gliding and parachuting performance of "flying" frogs were elucidated in experiments using physical models (Emerson and Koehl 1990; Emerson et al. 1990; McCay 2001). Physical models can also permit us to tease out the consequences of specific morphological features for several physical functions simultaneously. For example, Kingsolver and Koehl (1985, 1994) used physical models based on fossil insects to measure the effects of body size, wing length, and number of wings on both aerodynamic and thermoregulatory performance.

When models are used to analyze the performance of extant organisms, the biological relevance of a physical or mathematical model can be tested by comparing predictions of the model with the performance of the living organisms. For example, models of bipedal running were tested by comparing their predictions of the masses of leg muscles needed for rapid running with measurements for 10 extant species of bipedal runners (Hutchenson 2004). Similarly, drag measured on living sea anemones was not significantly different from drag measured on physical models of those individuals in the same postures when exposed to the same conditions of flow (Koehl 1977), and measurements of water velocity through the bristly feeding appendages of living copepods (planktonic crustaceans) matched those determined in experiments using physical models of those appendages (Koehl 2004). Glide angles measured in the field for living flying frogs matched those calculated from measurements of lift and drag on physical models (Emerson and Koehl 1990).

Mathematical and physical models of biomechanical function have not only been used to explore parameter space but also to test hypotheses about the function of, or to analyze mechanisms that could have been responsible for the performance of extinct organisms. For example, a finite element model of the stresses in the septae (dividing walls) in the shells of ammonites (extinct cephalopod mollusks) exposed to external pressure suggested rejection of the widely accepted hypothesis that ammonites with more complex septa were able to live at greater depths in the ocean than those with simpler septa (Daniel et al. 1997). Similarly, measurements of aerodynamic forces on models of extinct insects showed that the hypothesis that aerodynamic performance was an important factor in the elongation of short (relative to body length) protowings over evolutionary time should be rejected if ancestral insects were small (~2 cm body length), but not if they were large (~12 cm body length) (Kingsolver and Koehl 1985, 1994). Flow visualizations revealed the mechanism underlying this result: upward airflow around the tips of the wings rendered short wings ineffective at generating lift. Likewise, measurements of drag on and visualizations of water flow around physical models and shells of different types of cephalopods revealed how the size of the wakes that formed downstream of animals of different shapes affected drag, and thus, also affected estimates of their swimming performance (e.g., energetic cost, maximum velocity) (Chamberlain 1976, 1981). Experiments using robotic physical models of fossil clams that rocked back and forth in the sediment (as living clams do when burrowing) revealed that the mechanism responsible for the impressive burrowing performance of elongate shells with pointed posteriors and rounded anteriors was that the location of the axis of rotation shifted during different phases of the rocking motion such that the shell "walked" its way through the sediment (Stanley 1975).

Although the predictions of models of extinct organisms cannot be compared to the performance of those organisms, data about living organisms can be used to determine reasonable assumptions for the design of those models. For example, when Stanley (1975) used models of clams to study how the shapes of the shells of fossil species affected burrowing performance, he used kinematic analyses of films of burrowing behavior by living clams to determine how the model clams should be moved. Examples of using biomechanical analyses of locomotion in

extant birds to provide insights about and inform mathematical models of the locomotion of theropod dinosaurs and extinct birds were reviewed by (Hutchenson and Allen 2009).

Dynamically scaled physical models

In addition to the uses described above, physical models also provide a tool for investigating the functioning of organisms or the structures they build that are too large or too small to be conveniently manipulated or studied in the laboratory [reviewed by Vogel (1994) and Koehl (2004)]. For example, the effects of the shapes of the mounds around the openings to prairie dog burrows on wind-induced ventilation of these burrows was elucidated using small models in the lab (Vogel et al. 1973). Large models of the tiny feeding appendages of copepods (Koehl 1992, 1998, 2004) and of the arrays of microscopic chemosensory hairs on lobster olfactory antennules (Reidenbach et al. 2008) were used to study the detailed patterns of water flow around these structures as they capture food or odors, respectively. When such models are used to study velocities of flow around or through biological structures, or to determine the aerodynamic or hydrodynamic forces on them, the models should be dynamically similar to the bodies being modeled.

For studies of fluid dynamics, if a physical model and a biological structure are dynamically similar, then the ratios of the velocities and of the forces at comparable positions in the flow field around the model and around the real organism are the same. A model is dynamically similar to a biological structure if it is geometrically similar to the biological prototype, and if the relative importance of inertia and viscosity in determining flow patterns and forces on the structure is the same for the model as for the prototype. Reynolds number (*Re*) represents the relative importance of inertia to viscosity for a given flow situation:

$$Re = \rho UL/\mu \quad (1)$$

where U is speed of the fluid relative to the body, L is a linear dimension such as the structure's diameter, and ρ and μ are the density and dynamic viscosity, respectively, of the fluid. The models of the prairie dogs' burrows, copepods' appendages, and lobsters' antennules mentioned above were all operated at the same *Re*'s as their biological prototypes. The small models of burrows were exposed to water currents rather than to wind with velocities adjusted to achieve the right *Re*. The large models of microscopic appendages of arthropods were operated in viscous mineral oil rather than in water and were moved at very low velocities to match the *Re*'s of the real structures. Such large, slowly-moving models can also provide a useful way to study the fluid dynamics of structures such as flapping appendages of zooplankters (Koehl 1992, 1998, 2004) or insect wings (Dickinson et al. 1999; Usherwood and Ellington 2002) that move too rapidly to be studied easily on the real organisms.

In this article, we describe the design and use of physical models to study the gliding of extinct animals, using examples from our research on the feathered dinosaur, †*Microraptor gui*. Our goal is to provide a practical guide for others who might wish to incorporate this approach in their studies of the aerodynamics of gliding.

Example: designing physical models to study the aerodynamic performance of an extinct feathered dinosaur †*M. gui*

We have used dynamically scaled physical models to study the aerodynamic performance of the feathered theropod dinosaur, †*M. gui* (Fig. 1). Well-preserved fossils of †*M. gui*, a small dromaeosaur that lived during the early Cretaceous, have been discovered in the Jiufotang formation in Liaoning, China (e.g., Xu et al. 2003). Plant fossils in this formation indicate that †*M. gui* lived in a seasonally-varying diverse conifer-dominated forest habitat that also had other trees such as ginkoes and cycads, and herbaceous ground cover (Zhou et al. 2003; Zhou 2006; Benton et al. 2008).

†*Microraptor gui* had long pennaceous feathers with asymmetrical vanes (features characteristic of flight feathers on modern birds) on the distal segments of its hind limbs, as well as its forelimbs, and it had a long feathered tail (Xu et al 2003; Chatterjee and Templin 2007; Witmer 2009). Because its foot morphology was consistent with perching and climbing and because it had long feathers on its feet that might have made running difficult, †*M. gui* has been interpreted to be an arboreal animal (Prum 2003; Xu et al. 2003; Zhou et al. 2003). A variety of aerodynamic functions have been suggested for the feathered hind limbs of †*M. gui*, including serving as lift-generating wings (e.g., Prum 2003; Xu et al. 2003; Chaterjee and Templin 2007; Alexander et al. 2010), functioning as air brakes or flight maneuvering surfaces (Paul 2003; Zhang and Zhou 2004), reducing air resistance on the legs by streamlining them (Zhou and Zhang 2005; Chatterjee and Templin 2007), or increasing drag on the animal to reduce the speed of a fall (Padian 2003).

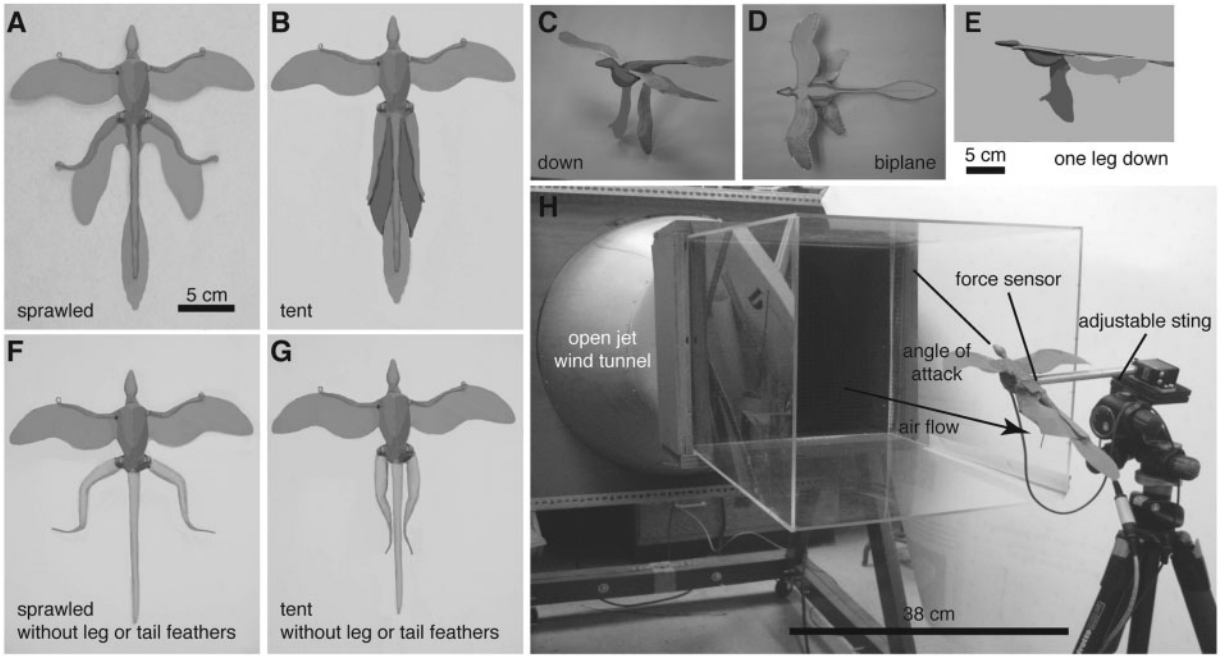

Fig. 1 Diagrams of models of †*Microraptor gui* in a variety of configurations (**A–G**). Various postures that have been proposed for †*M. gui* were tested using models with feathers on forelimbs, hind limbs, and tail: (A) sprawled, (B) tent (legs back with their feathers forming a tent over the tail), (C) down, and (D) biplane (knees bent such that the distal portions of the leg wings are lower than the arm wings). (E) Different asymmetric postures that might have been used to execute maneuvers, such as the one illustrated here, were tested. The effects of aerodynamic surfaces aft of the center of mass were studied by comparing fully-feathered models (A–E) with models that had feathers on forelimbs but not on hind limbs or tail (F and G) in various postures including those illustrated here: (F) sprawled and (G) legs back. (H) Photograph of a model of †*M. gui* in the tent posture in the open-jet wind tunnel (working section 0.381 m × 0.381 m in cross-section and 0.457 in length). The model has paper feathers. The angle of attack (α) is the angle between the direction of airflow relative to the body and the long axis of the body. A force transducer (ATI Nano17-6DOF force/torque sensor) was mounted in the model's torso at the center of mass of the model. A, B, F, and G are ventral views, and D is a dorsal view.

Nonaerodynamic functions such as signaling have also been proposed for leg feathers (Padian 2003; Paul 2003), but even if the selective factors that led to the initial evolution of long feathers on the legs did not relate to flight, those feathers would have had aerodynamic consequences (Witmer 2009). Therefore, †*M. gui*, with its feathered hind limbs, is of interest both to biomechanists studying the designs of gliding organisms and to evolutionary biologists trying to unravel the origins of flight in the ancestors of birds.

While gliding birds and man-made gliders have their wings anterior to or near their center of mass (e.g., Pennycuick 1972), some gliding animals such as "flying frogs" have large aerodynamic surfaces (big webbed feet) posterior to their center of mass. Flying frogs are poor gliders (i.e., do not travel very far horizontally per vertical distance of fall) but are more maneuverable than are frogs that do not have the flyer's morphology of enlarged webbed feet (Emerson and Koehl 1990; McCay 2001). Frogs maneuver by changing the positions and angles of their feet, and their aerodynamically-unstable bodies do not resist such maneuvers (McCay 2001). The large feathered hindwings of †*M. gui* might have contributed to maneuverability in a similar fashion. However, unlike frogs, †*M. gui* also had large forewings and a long feathered tail (Fig. 1A). Therefore, the aerodynamic properties of of †*M. gui* can provide insights about maneuverability and gliding performance of bodies with large surfaces posterior to the center of mass.

The discovery of †*M. gui*, a forest-dwelling dinosaur with "wings" on its legs, added fuel to the lively debate about the origin of flight in the feathered dinosaur ancestors of birds (reviewed by Homberger 2003; Prum 2003; Zhou 2004; Hutchenson and Allen 2009; Ruben 2010). The "ground-up" school of thought argues that the ancestors of birds were ground-dwelling dinosaurs and that flapping of feathered forelimbs enhanced their running ability, eventually leading to powered take-off and flight. Evidence and arguments in favor of this hypothesis are given by Ostrom (1986), Padian and Chiappe (1998), Burgers and Chiappe (1999), Bundle and Dial (2003), Dial

(2003), Hutchenson (2003), Dial et al. (2006, 2008), and Peterson (this symposium). Evidence and arguments against this hypothesis are given by Senter (2006), and Nudds and Dyke (2009). The "trees-down" point of view argues that the ancestors of birds were arboreal and that aerodynamic feathered surfaces improved their performance while parachuting or gliding through the forest, eventually leading to arm flapping and powered flight. Evidence and arguments in favor of this hypothesis are given by Norberg (1985), Bock (1986), Xu et al. (2000, 2003, 2005), Long et al. (2003), Paul (2003), Zhang and Zhou (2004), Chatterjee and Templin (2007), and Alexander et al. (2010). Evidence and arguments against this hypothesis are given in Padian (2003), and Padian and Dial (2005). Phylogenetic analyses of the theropod dinosaurs and of birds (e.g., Norell and Xu 2005; Kurochkin 2006; Longrich 2006; Hu et al. 2009; Hutchenson and Allen 2009) indicate that †*M. gui* was not part of the lineage of theropods leading to birds (the Avialae), but rather, was part of a sister group with feathered legs (the Dromaeosauridae). The "ground-up" camp argue that the common ancestor of both lineages had only forewings, and that hindwings developed in the lineage leading to †*M. gui* (e.g., Padian 2003), whereas the "trees-down" proponents argue that the common ancestor of both lineages had four wings, but the rear wings were lost in the lineage that led to birds (e.g., Beebe 1915; Prum 2003; Xu 2003; Zhang and Zhou 2004; Hu et al. 2009). Although an aerodynamic analysis of †*M. gui* cannot resolve this debate, it can provide information about the performance of this animal while airborne and also can tease out the effects of the feathered legs and a long, feathered tail on aerodynamic function.

Several modeling studies have been conducted of †*M. gui* to explore its gliding performance. Chatterjee and Templin (2007) used computer simulations of airflow around and forces on †*M. gui* in the "biplane" posture (Fig. 1D) to calculate its gliding performance and concluded that †*M. gui* was a "moderate" glider (i.e., its horizontal speed relative to its sinking speed was lower than those calculated for a frigate bird and a pterosaur), that its glide path would have undulated up and down, and that its long tail could have stabilized it during gliding. Alexander et al. (2010) measured the glide trajectories of life-sized physical models of †*M. gui,* but with a bilobed tail at an angle of 20° above the frontal plane of the body, and tested models with the legs in three postures: (1) legs held out to the side (Fig. 1A), but tilted in an anhedral configuration at an angle of 20° below the frontal plane, (2) posture (1), but with the distal portion of each leg parallel to the plane of the forelimb wings, and (3) biplane posture (Fig. 1D). Alexander et al. (2010) found that †*M. gui* in postures (1) and (2) was a stable glider with a mean lift-to-drag ratio of ~4, but that †*M. gui* in the biplane posture was unstable (unless a heavy counterweight was put in the head) and showed slightly worse gliding performance. The lift and drag forces (Fig. 2A) on a life-sized model of †*M. gui* with its legs in various postures, including "tent" (Fig. 1B and H), "down" (Fig. 1C), biplane (Fig. 1D), and tucked up under the body, were measured in a wind tunnel (NOVA television program "The Four-Winged Dinosaur", aired by Public Broadcasting System on February 26, 2008; directed by Mark Davis, model constructed by Hall Train, and measurements made in the wind tunnel by Arnold Song, Kenneth Breuer, Joseph Bahlman, Steve Gatesy, Farish Jenkins, Mark Norell, and Xu Xing). These experiments suggested that the tent posture yielded the best gliding performance (highest lift-to-drag ratio).

We have been using physical models of †*M. gui* to explore more postures than those investigated in the earlier modeling studies, including asymmetric arm and leg configurations and tail positions that could have been used in executing maneuvers (e.g., Fig. 1E). In addition, we have been comparing the performance of models with and without leg and tail feathers (Fig. 1F and G) to investigate the roles of large aerodynamic surfaces posterior to the center of mass. We have also been exploring other types of aerodynamic performance (listed below) in addition to the aspects of gliding that were the focus of the modeling studies cited above. As the purpose of the present article is to discuss how to design and test dynamically scaled physical models for investigating the gliding mechanics of extinct organisms, the results of the experiments in which asymmetric postures or plumage were varied will be reported elsewhere.

Designing a physical model that is geometrically similar to †*M. gui*

A dynamically scaled physical model must be geometrically similar to the biological prototype. There are challenges to designing such a model when the only records of the morphology of an organism are fossils of skeletons and other hard body parts that can be flattened or distorted (Briggs et al. 1991). If logistically possible, careful examination of the fossils and consultation with the paleontologists who study them is recommended, in addition to study of the

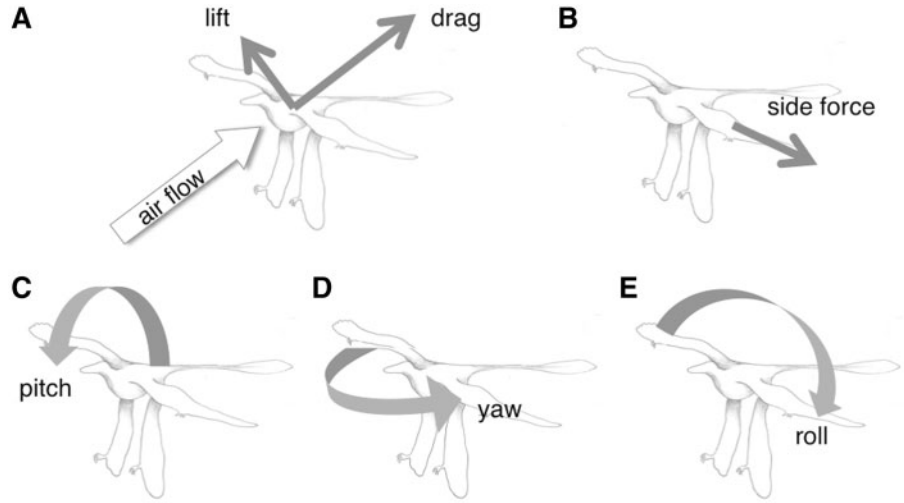

Fig. 2 (**A**) Drag is the aerodynamic force acting in the same direction as the airflow relative to the body (+ drag is in the direction of that airflow), and lift is the force acting at right angles to the drag in the dorso-ventral direction (+ lift is upward). (**B**) Side force is the aerodynamic force acting at right angles to drag and to lift in the left–right direction (+ side force is toward the right). (**C**) Pitch is rotation of the body in the nose-up (+) or nose-down direction (−). (**D**) Yaw is rotation of the body in the nose-right (+) or nose-left (−) direction. (**E**) Roll is rotation of the body about its long axis in the right-wing-down direction (+) or right-wing-up direction (−).

published descriptions, photographs, and reconstructions of the fossils. It is also helpful to learn about the morphology of related extinct and extant organisms.

One important issue to resolve is the shape of the animal when the soft tissues were present. A common way to proceed is to construct a skeleton from casts of the fossil bones, to flesh it out with muscles based on the anatomy of living related organisms (e.g., birds for †*M. gui)*, and to cover it with feathers that match the fossil feathers in type, size, and number (e.g., Davis et al. 2008, NOVA show cited above; Alexander et al. 2010). To do the latter, assumptions must be made about the orientation of the feathers and the stiffness of their attachment to the integument (Padian 2003). In our study, we based the body shape of, and arrangement of feathers on our models on the reconstruction of †*M. gui* in the published description of the fossils (Xu et al. 2003).

Another challenge in constructing a geometrically-similar model of a fossil organism is to determine the posture(s) in which to configure the body. The fossil skeleton can become distorted during preservation, so there are different interpretations of how the hip joints of †*M. gui* constrained possible positions of the legs (Prum 2003; Fucheng et al. 2006). The original reconstruction of the fossil showed the legs sprawled laterally (Fig. 1A; Xu et al. 2003). While some researchers argue that the hip joints of related theropod dinosaurs and of birds do not permit the thighs to be positioned laterally and thus the sprawled posture was unlikely (e.g., Padian 2003; Padian and Dial 2005; Chatterjee and Templin 2007), others argue that some versions of the sprawled posture are feasible (e.g., Hertel and Campbell 2007; Alexander et al. 2010). Various configurations of the legs that theropods' hip and leg joints could have permitted have been suggested, including the legs-down posture (Fig. 1C), biplane posture (Chatterjee and Templin 2007; Fig. 1D), and tent posture (Fig. 1B and H). One advantage of using physical models is that they permit us to try all of the proposed postures to see if they make any difference to aerodynamic performance. We tested our models in each of the above postures, as well as, in various asymmetric ones (Fig. 1).

Determining the *Re* of an extinct organism

Dynamically scaled physical models operate at or near the *Re* ($Re = LU\rho/\mu$) of the real organism. The linear dimensions of †*M. gui* can be measured on the fossils, or on photographs or diagrams of the fossils (Xu et al. 2003), but the speed (U) of †*M. gui* falling through the air must be estimated and the density (ρ) and viscosity (μ) of the air at the time that they lived must be determined.

Although wing length (base to tip), chord length (anterior to posterior length of a wing), or body length can be used for L in calculations of *Re*, we chose to use snout–vent length because it does not change for different postures (McCay 2001) or experimental removal of feathers and because it is a standard biological scale of length used for reptiles.

The engineering convention for winged aircraft is to use chord length for *L*. We measured snout–vent length on the photographs and diagram of †*M. gui* in Fig. 1 of Xu et al. (2003) and found it be 0.30–0.32 m, depending on where we assumed the vent to be located.

One way to estimate the speeds of extinct organisms is to assume that they moved within the range of speeds used by living organisms of similar mass and wing loading (*W*):

$$W = mg/S \quad (2)$$

where m is the mass of the organism, g is the acceleration due to gravity (9.81 m/s^2), and *S* is the planform area (e.g., Alexander 1982). In engineering analyses of wings and winged aircraft and in most studies of the aerodynamics of birds, *S* represents the planform area of the wings alone. However, for organisms without wings, such as gliding snakes (Socha and LaBarbera 2005) and frogs (Emerson and Koehl 1990), the planform area of the whole body is used for *S*. In the case of †*M. gui,* we used the planform area of the whole body for *S* because the feathered area of the hind limbs and tail is as big as that of the wings and because we manipulated those areas in our experiments.

Various approaches have been used to determine the mass of an extinct organism, including measuring the volume of water displaced by a model of the organism and then multiplying that volume by an assumed tissue density (e.g., Peczkis 1994; Christiansen and Farina 2004; Alexander et al. 2010), using bivariate or multivariate regressions for modern vertebrates of body mass as a function of specific bone dimensions that can also be measured on the fossils (e.g., Christiansen and Farina 2004) or digitizing the outer surface of a reconstruction of the organism and then summing the masses of slices of the body computed using assumed tissue densities (Henderson 1999; Hurlburt 1999). The latter technique can account for body regions with different densities (e.g., air-filled lungs, dense bones) if the coordinates of their outer surfaces can be measured. The body mass of †*M. gui* has been estimated to be 0.95 (Chatterjee and Templin 2007) to 1.23 kg (Alexander et al. 2010) and the wing loading to be 70.6 N/m^2 (Chatterjee and Templin 2007). Examples of published airspeeds for gliding birds, bats, and reptiles of similar mass (Table 1) range from 6.1 to 14.2 m/s. Gliding speeds of †*M. gui* have been estimated to be 10.6 m/s by Alexander et al. (2010) using the relationship between air speed and *W* proposed by Tennekes (1996) and to be 12–15 m/s by Chaterjee and Templin (2007) using computer simulations of gliding by †*M. gui.* Therefore, we estimated that a reasonable range of possible *U*'s for †*M. gui* was 6–15 m/s.

The composition of the atmosphere during the early Cretaceous when †*M. gui* lived was very similar to its composition today (Dudley 1998; Berner et al. 2003). Because †*M. gui* lived in temperate forests, we assumed air temperatures of 10–20° C and used the viscosity ($\mu = 1.7 \times 10^{-5}$ at 10°C and 1.8×10^{-5} kg m^{-1} s^{-1} at 20°C) and the density ($\rho = 1.2$ kg m^{-3} and at both 10 and 20° C) of dry air at sea level in our calculation of *Re* (e.g., Vogel 1994; Haynes and Lide 2011). Elevation has a small effect on the density and viscosity of air (e.g., at an elevation of 2000 m at 20°C, $\rho = 1.0$ kg/m^3 and $\mu = 1.7 \times 10^{-5}$ kg m^{-1} s^{-1}), as does relative humidity

Table 1 Mass, wing loading [Equation (2)], and gliding speeds for various animals

Animal	Mass (kg)	Wing loading (N/m^2)	Gliding speed (m/s)
†*Microraptor gui*	0.95 (Chatterjee and Templin (2007)	70.6 (Chatterjee and Templin (2007)	12 to 15 (Chatterjee and Templin (2007)
	1.23 (Alexander et al. 2010)		10.6 (Alexander et al. 2010)
Buzzard	1.0 (Tennekes 1996)	37 (Tennekes 1996)	9.9 (Tennekes 1996)
Red-tailed hawk	1.1 (Tennekes 1996)	54 (Tennekes 1996)	11.7(Tennekes 1996)
Roseate spoonbill	1.3 (Tennekes 1996)	57 (Tennekes 1996)	12.3 (Tennekes 1996)
Frigate bird	1.5 (Chatterjee and Templin (2007)	45 (Chatterjee and Templin (2007)	10 (Chatterjee and Templin (2007)
Harris hawk	0.70 (Rosen and Hendenstrom 2001)		6.1 (Rosen and Hendenstrom 2001)
Laggar falcon	0.57 (Rosen and Hendenstrom 2001)		6.6 (Rosen and Hendenstrom 2001)
Pteropus sp. (bat)	0.65 (Norberg et al. 2000)	25.8 (Norberg et al. 2000)	9.8 (Norberg et al. 2000)
Chrysopelea ornate (gliding snake)	0.24 (Heyer and Pongsapipatana 1970)		14.2 (Heyer and Pongsapipatana 1970)

(e.g., at a relative humidity of 50% at sea level at 20° C, $\rho = 1.2\,kg/m^3$ and $\mu = 1.7 \times 10^{-5}\,kg\,m^{-1}\,s^{-1}$) (Pennycuick 1972; Benson 2009; Haynes and Lide 2011).

Using the estimates of L, U, ρ, and μ described above, we calculated the range of possible Re's at which †*M. gui* might have operated to be about 1×10^5 to 3×10^5.

Quantifying aerodynamic performance of a gliding organism

We measured aerodynamic forces and moments on physical models of †*M. gui* in a wind tunnel (Fig. 1H) using a six-axis force transducer (Nano17, ATI Industrial Automation) affixed in the model's torso at its approximate center of mass. The transducer was mounted on a threaded steel rod damped with rubber tubing. The mounting rod exited the right side of the model and was attached to a tripod that was used to change the model's angle of attack (α, the angle between the direction of airflow relative to the model and the frontal plane of the model; Fig. 1H). By convention in engineering studies of aircraft, α is the angle between the chord of the wing and the direction of airflow. For organisms with no wings or with many wings (each of which can be at a different α), biologists must make clear which part of the body is being used to measure α. In the experiments with †*M. gui* reported here, the chords of the forewings were parallel to the frontal plane of the body, so one α describes the orientation both of body and wings with respect to the airflow.

As a body moves through the air, the airflow relative to the body is the same speed, but in the opposite direction as the velocity of the body. Therefore, we could simulate the airflow encountered by a freely-gliding †*M. gui* by exposing a stationary model to airflow in an open-jet wind tunnel (described by McCay 2001). Air speeds encountered by our models were measured using a hot wire anemometer (Series 2440, Kurz Instrument Co.). The outputs from the force transducer were recorded at a sampling frequency of 1000 Hz using a National Instruments 6251 data-acquisition card. For each replicate experiment, the forces and moments recorded for a 3-min period were averaged after being rotated from the frame of reference of the model into the frame of reference of the laboratory (scripts in Python). Various indices of performance could then be calculated from these measurements of forces and moments. These performance indices are described in aerodynamics texts (e.g., McCormick 1995; Etkin and Reid 1996) and are summarized and explained for biologists by Emerson and Koehl (1990), Vogel (1994), and McCay (2001).

We measured drag (aerodynamic force parallel to the direction of airflow relative to the body; Fig. 2A), lift (aerodynamic force perpendicular to the drag in the dorso-ventral direction; Fig. 2A), and side force (aerodynamic force perpendicular to the drag and lift acting in the left–right direction; Fig. 2B), as well as, the moments in pitch (Fig. 2C), yaw (Fig. 2D), and roll (Fig. 2E). We used those measurements to calculate coefficients that are dimensionless indices of the effects of body shape and orientation on aerodynamic forces and moments: C_D (coefficient of drag), C_L (coefficient of lift), C_S (side force coefficient), C_m (pitching coefficient), C_n (yawing coefficient), and C_r (rolling coefficient).

$$\text{Drag} = 0.5\ C_D \rho\ (S)\ (U)^2 \tag{3}$$

$$\text{Lift} = 0.5\ C_L \rho\ (S)\ (U)^2 \tag{4}$$

$$\text{Side force} = 0.5\ C_s\ \rho\ (S)\ (U)^2 \tag{5}$$

$$\text{Pitching moment} = 0.5\ C_m \rho\ (S)\ U^2 L \tag{6}$$

$$\text{Yawing moment} = 0.5\ C_n \rho\ (S)\ U^2 L \tag{7}$$

$$\text{Rolling moment} = 0.5\ C_r \rho\ (S)\ U^2 L \tag{8}$$

where S is the planform area of the body and L is a linear dimension of the body. We measured S by digitizing photographs of models (using Image J software) in the sprawled position because in this posture the feathered surfaces are parallel to the plane measured and none are hidden behind other parts of the body (see Fig. 1A). As explained above, we used snout–vent length for L for our models of †*M. gui*. In the engineering literature, chord length is used for L in Equation (6), and wingspan is used for L in Equations (7) and (8) (e.g., McCormick 1995).

Parachuting

The more slowly a falling body moves, the longer it can remain airborne and the softer its landing (the magnitude of the force with which an animal of a given mass hits the ground or some other object in its environment is proportional to its speed at the time of impact, so more slowly-moving organisms are less likely to be injured when landing). The time aloft for a falling body is proportional to $(\text{drag/m})^{1/2}$ (Norberg 1985), so the maximum drag coefficient, $[(C_D)_{max}$, which for most bodies occurs

at $\alpha = 90°$], can be used as a measure of its parachuting performance (e.g., Emerson and Koehl 1990).

Gliding

One standard measure of gliding performance is the horizontal distance traveled per height lost as an animal falls, which is proportional to the ratio C_L/C_D (e.g., Pennycuick 1972). Since both C_L and C_D (Equations (3) and (4) depend on α, C_L/C_D is determined for a range of α's and the highest lift-to-drag ratio achieved, $(C_L/C_D)_{max}$, is typically used to characterize the gliding performance of a body (e.g., Pennycuick 1972; Emerson and Koehl 1990; Vogel 1994).

Another aspect of gliding performance is the minimum airspeed (U_{min}) that must be attained by a falling body to generate sufficient lift to begin gliding. When an animal starts falling through the air, it accelerates. The lower the U_{min}, the sooner after take-off an animal can begin to glide, and thus the greater the proportion of its time aloft can be spent travelling horizontally. Minimum glide speed is given by (Alexander 1982):

$$U_{min} = \left[\frac{2W}{C_L}\right]^{1/2} \quad (9)$$

where W is the wing loading [Equation (2)], ρ is the fluid density, and C_L is the lift coefficient [Equation (4)].

Stability

When organisms fall through the air in nature, they can be buffeted by turbulent wind or tipped by objects or other organisms in their environment. Therefore, their stability when hit by such perturbations is another aspect of aerodynamic performance that might affect their survival. If a body in a given configuration shows static aerodynamic stability, then there is an orientation at which the body experiences no moment (stable fixed point; Fig. 3B) and the moments about its center of mass if it is perturbed (e.g., if its orientation is altered by a wind gust) act in the opposite direction of that perturbation and tend to push the body back to its original stable orientation without requiring any active righting behavior. The slope of a plot of the moment on a body as a function of angle of orientation is negative if the body is stable. In contrast, if a body is unstable, there is an orientation at which the body experiences no moment (unstable fixed point, Fig. 3C), but if it is perturbed from that orientation, the moment on the body acts in the same direction as the perturbation and can cause the body to tumble. The slope of a plot of the moment on a body as a function of angle of orientation is positive if the body is unstable. If a body shows neutral stability, then no moments are set up on the body in the perturbed orientation, so the body remains in a new orientation after the perturbation stops. If a body is neutrally stable, the slope of a plot of the moment on a body as a function of angle of orientation is zero and the magnitude of the moment is zero, so it experiences no stabilizing or destabilizing moments if perturbed to a new orientation.

The bigger the change in pitching (Fig. 2C), moment produced by a given change in angle of attack (α, Fig. 1H) of a body, the more stable the body is if that moment acts in the opposite direction from the change in α. Conversely, if that moment acts in the same direction as the change in α, then the body is more unstable if the change in pitching moment per change in α is large. Therefore, a measure of the static aerodynamic pitching stability of a body is the pitching stability coefficient, $C_{m,\alpha}$, given by:

$$C_{m,\alpha} = \partial C_m/\partial\alpha \quad (10)$$

where C_m is the pitching coefficient [Equation (6)], and α is the pitch angle or angle of attack (Fig. 1H). If $C_{m,\alpha}$ is positive, the body is unstable, if $C_{m,\alpha}$ is negative, the body is stable, and if $C_{m,\alpha} = 0$, the body is neutrally stable. Since C_m can depend on α, we determine C_m/α by taking the local slope of a plot of C_m as a function of α.

Similar stability coefficients can be used for yaw (Fig. 2D) and roll (Fig. 2E) (McCay 2001). The yawing stability coefficient $C_{n,\Psi}$, is given by:

$$C_n,\Psi, = \partial C_n/\partial\Psi \quad (11)$$

where C_n is the yawing coefficient [Equation (7)] and Ψ is the yaw angle (angle between the anterior–posterior axis of the body and the direction of airflow relative to the body). The rolling stability coefficient, $C_{r,\Phi}$, is given by:

$$C_r,\Phi = \partial C_r/\partial\Phi \quad (12)$$

where C_r is the rolling coefficient [Equation (8)] and Φ is the roll angle (angle between the dorso-ventral axis of the body and vertical). For pitch, yaw, and roll, we use the sign conventions outlined by McCay (2001) (Fig. 2).

When an organism executes a maneuver, it changes its orientation. The aerodynamic forces on stable bodies produce a moment acting in the opposite direction from the moment of the maneuver and

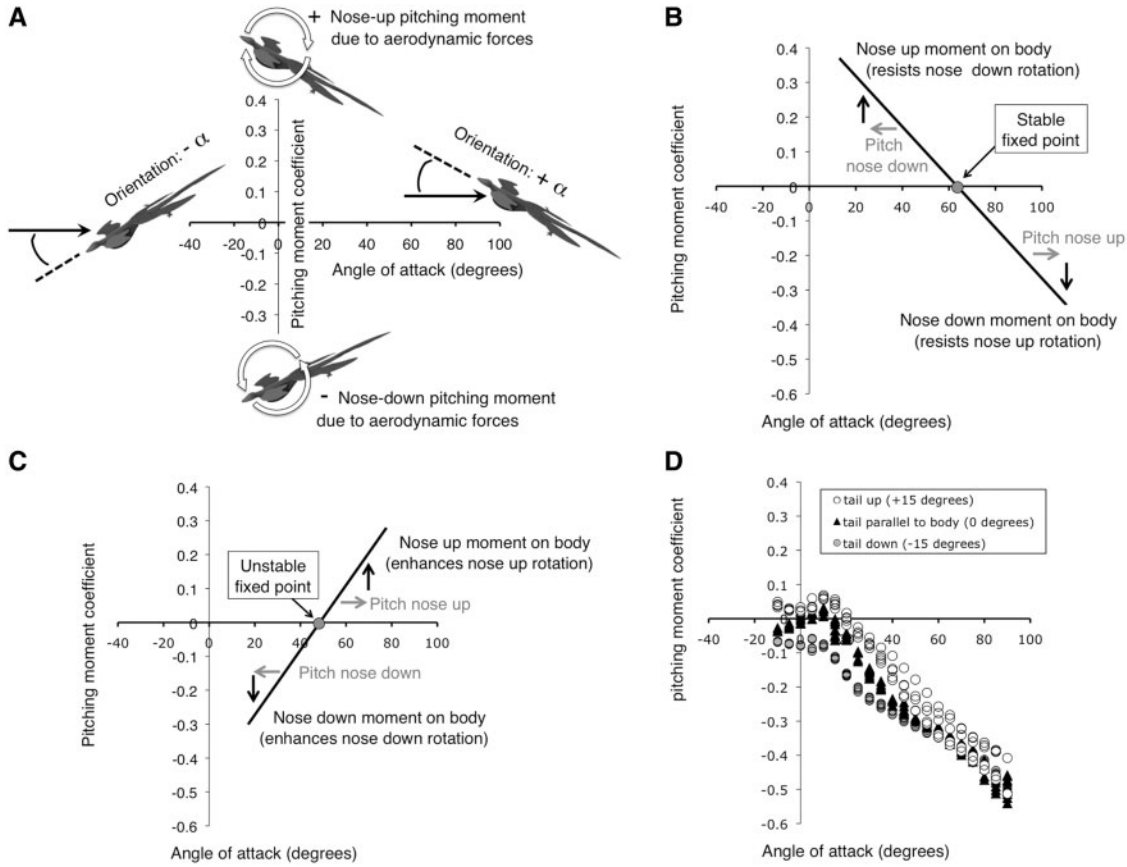

Fig. 3 Pitching moment coefficient plotted as a function of angle of attack. (**A**) Diagrams explaining the axes of the graphs in B–D. Angle of attack (α, angle between the frontal plane of the body and the direction of airflow relative to the body, indicated by black arrow) is plotted on the horizontal axis. A positive α indicates a nose-up orientation from the direction of airflow relative to the body, and a negative α indicates a nose-down orientation. The coefficient [C_m, Equation (6)] of the pitching moment imposed on the body by the airflow it experiences at each α is plotted on the vertical axis, where a positive coefficient indicates a nose-up moment, and a negative coefficient indicates a nose-down moment. (**B**) Example of the behavior of a body that shows static aerodynamic stability in pitch. (**C**) Example of a body that shows static aerodynamic instability in pitch. (**D**) Pitching moment coefficient plotted as a function of α for models of †*M. gui* in the sprawled posture. Each symbol represents an independent replicate measurement. Black triangles indicate measurements for the model when its tail is parallel to the long axis of the body, open circles when the tail is raised at an angle of 15° above the long axis of the body, and gray circles when the tail is 15° below the long axis of the body. The sprawled posture with its tail at 0° has a stable equilibrium point near an α of 10° angle-of-attack, and an unstable fixed point at an α of around 0°. Tail movement upward alters the stable position to an α of about 20°, whereas, tail movement downward changes stability entirely. The vertical spread between the plots for the different tail orientations indicates the control effectiveness of the tail.

thus, resist that maneuver. In contrast, when an unstable body executes a maneuver, the aerodynamic forces on it produce a moment that acts in the same direction as the moment of the maneuver and thus, augments the maneuver. However, an unstable animal will continue to spin or tumble unless it actively stops the rotation. Even for bodies that are not stable or unstable (i.e., have no fixed points at which the moment they experience is zero), the local slope of a plot of the coefficient of the moment on the body as a function of body angle (i.e., the local stability coefficient) reveals whether the aerodynamic forces on the body with that orientation resist or augment a maneuver that changes body angle.

An example of how the pitching moment on a body in a defined posture can either resist or augment a pitching maneuver, depending on the body's orientation relative to the flow, is illustrated in Fig. 3D. The pitching moment on a model of †*M. gui* with its hind limbs in the sprawled posture is plotted as a function of angle of attack (α) for different orientations of the tail. When the tail is held parallel to the anterior–posterior axis of the body (black triangles), it experiences zero moment at an α of approximately 10°. At this fixed stable point, the slope of the plot is negative, indicating that the body should experience restoring moments when perturbed away from this stable point.

The animal should be difficult to maneuver in the range of α's for which the slope is negative. †*Microraptor gui* in this posture also experiences zero moment at an α of 0°, but there the slope is positive, indicating that if the body is perturbed away from this unstable fixed point, the moment on it will act in the same direction as the perturbation. Therefore, in the range of α's around 0°, where the local slope is positive, †*M. gui* should be easier to maneuver than at higher α's, where the slope is negative.

Maneuverability

If a parachuting or gliding animal is maneuverable, it can quickly alter its course to steer to a desired landing site, to avoid collisions with objects such as trees, or to dodge, intercept, or display for another animal (e.g., predator, prey, competitor, mate). A statically-stable body resists changes in orientation that are actively imposed by the animal as well as those caused by environmental perturbations. Thus, there is a trade-off between aerodynamic stability and maneuverability, and unstable animal bodies can be more easily maneuvered than stable ones (e.g., Maynard-Smith 1952; Emerson and Koehl 1990; McCay 2001).

Aerodynamic maneuverability is not only affected by body stability, but also depends on the effectiveness of control surfaces at generating moments when they change their orientation, shape, or position. Dimensionless indices of the control effectiveness of an appendage (such as a tail, leg, or wing) indicate how big a moment can be generated for a given change in the appendage. The control effectiveness coefficient for pitch, $C_{m,\delta}$, is given by:

$$C_m,\delta = \partial C_m/\partial\delta \quad (13)$$

where C_m is the pitching coefficient [Equation (6)] and δ is an angle describing the orientation, position, or configuration of the appendage (e.g., a joint angle, or an angle of a control surface with respect to a defined plane). The control effectiveness coefficient for yaw, $C_{n,\delta}$, is given by:

$$C_n,\delta = \partial C_n/\partial\delta \quad (14)$$

where C_n is the yawing coefficient [Equation (7)]. The control effectiveness coefficient for roll, $C_{r,\delta}$, is given by:

$$C_r,\delta = \partial C_r/\partial\delta \quad (15)$$

where C_r is the rolling coefficient [Equation (8)].

If a gliding animal rolls, the lift on its body has a sideways component that enables the animal to execute a banking turn. The turning radius (r) of a banking glider is given by (Pennycuick 1971):

$$r = 2W/(\rho C_L \sin\Phi) \quad (16)$$

where W is wing loading [Equation (2)], ρ is the fluid density, C_L is the coefficient of lift [Equation (4)], and Φ is the roll angle or banking angle. Therefore, for a given Φ, tighter turns (i.e., turns with lower r's) can be executed by animals with higher C_L/W. Since C_L varies with α, $(C_L/W)_{max}$ can be used as a measure of the best turning performance of a banking animal (Emerson and Koehl 1990).

An example of the effectiveness of the tail in controlling pitch for †*M. gui* is illustrated in Fig. 3D. If the animal swings its tail up (open circles), the nose should pitch upward. However, in the case of †*M. gui* in the sprawled posture, the aerodynamic forces on the large feathered hind wings (which pitch the nose down) are so large that the nose-up (positive) moment due to the tail simply reduces the nose-down (negative) moment on the model. In contrast, if the tail is deflected down (gray circles), the body experiences a greater negative (nose down) pitching moment. The vertical spread between the plots for the different orientations of the tail shows in a general sense the control effectiveness of the tail. An alternative way to look at this plot is to examine the shift in the stable equilibrium point when the position of the tail is changed. For example, the new stable α for the tail-up posture is approximately 20°. In contrast, for the tail-down posture, there is no new stable point and the animal would eventually tumble.

Practical constraints and considerations

Available equipment

The equipment available to a researcher can impose constraints on the design of physical models. For example, Vogel (1985, 1987) used air rather than water in studies of pressure distributions around models of marine organisms because he had a pressure transducer that worked in air, but not in water. Similarly, Kingsolver and Koehl (1985) used water rather than air for analyzing the flow around dynamically scaled models of fossil insects because we had a dye system for visualization of flow in water, but no equipment for visualizing airflow.

In our study of †*M. gui*, the working sections of the available wind tunnel limited the size of the models we could use, hence we constructed models smaller than †*M. gui*, but exposed them to higher airspeeds than those we estimated for the animal,

so that we could achieve the same *Re*. Another technical constraint that we faced was that the maximum air speeds attainable in our wind tunnel did not permit us to test the higher *Re*'s of the range we estimated for †*M. gui* (see above): the highest *Re* we could produce in our wind tunnel (7×10^4) was of the same order as the lowest estimated *Re* for †*M. gui* (1×10^5). However, bluff bodies have roughly constant C_D's in the range of *Re*'s between $\sim 10^3$ and $\sim 4 \times 10^5$ and streamlined bodies have constant C_D's to even higher *Re*'s (e.g., Hoerner 1965; Vogel 1994). We measured the aerodynamic forces on our models for the range of *Re*'s that we could test in our wind tunnels and found C_D and C_L to be constant (e.g., Fig. 4). Tucker (1990) found constant C_D's for a number of species of birds in this same *Re* range. Although we cannot extrapolate beyond our data, a reasonable assumption would be that C_D and C_L of †*M. gui* would also be independent of *Re* in the *Re* range of 1.0×10^5 to 3×10^5 that we estimated for †*M. gui*.

Ease of fabrication and durability of models

Physical models can be fabricated using a variety of materials and techniques. Although the material properties of the organism should be replicated in a model, we can only make educated guesses about the material properties of extinct organisms based on properties of similar structures in extant species. It is also desirable to construct a durable model so that replicate measurements can be made. For example, Alexander et al. (2010) found that a foam model of †*M. gui* bearing real feathers was too fragile for repeated free-gliding experiments, and replaced it with more durable models constructed of plywood and metal with balsa-wood plumage. Similarly, after initially experimenting with delicate wire and foam models of †*M. gui*, we switched to more durable models of the body made from a polymer clay (Super Sculpey Firm, Polyform Products Co.) supported by an aluminum torso and steel-rod skeletons in the appendages. In addition, some details of the organism can be very time-consuming to replicate on a model. Therefore, it can be worthwhile to determine whether such features as material properties or details of texture affect the aspects of performance to be measured. Our first models had real bird feathers on forelimbs, hind limbs, and tail (Fig. 5A) to approximate the surface texture of †*M. gui*, Each feather used was matched in size to a feather on a diagram of the fossil (Xu et al. 2003) that had been scaled to the size of the model. However, we found that replicate models could be constructed much more rapidly by replacing the rows of individual feathers with more durable sheets of paper cut to the shape of the feathered surfaces on forelimbs, hind limbs, and tail, and reinforced with monofilament line (Fig. 1H). By comparing the aerodynamic forces on the models with real feathers versus those with paper plumage, we found that performance of the durable, easily manufactured model was not significantly different from that of the feathered model (e.g. Fig. 5B).

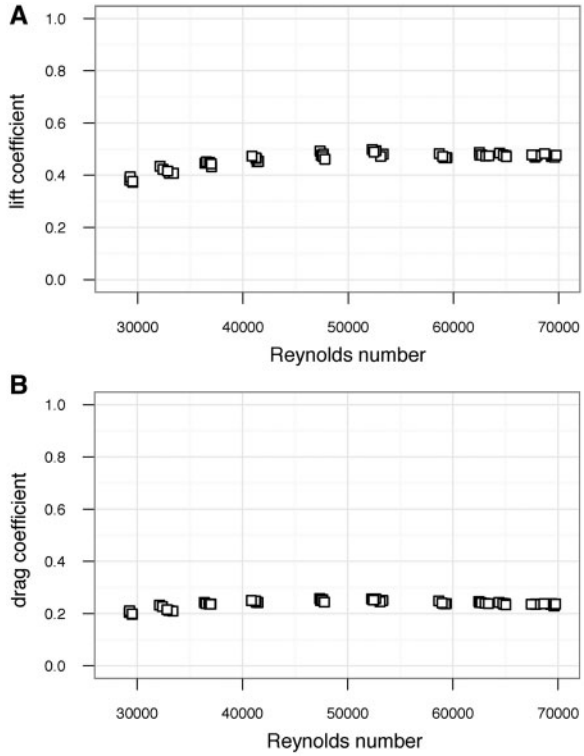

Fig. 4 Lift coefficient (**A**) and drag coefficient (**B**) plotted as a function of *Re* for models of †*M. gui* in the tent posture. Each symbol represents an independent replicate measurement. There were no significant differences between the lift coefficients measured at different *Re*'s, and there were no significant differences between the drag coefficients measured at different *Re*'s (ANOVA, $P > 0.05$).

Determining center of mass

The stability and control effectiveness indices above are defined based on the center of mass (COM) of the organisms, and it is often best to measure aerodynamic forces and moments about the COM. To locate the COM for an extant species, a preserved specimen of the body can be cut into small pieces, each of which is weighed. Then the distribution of mass in the model can be designed to replicate that of the real organism (technique described by Emerson and Koehl 1990). For extinct organisms,

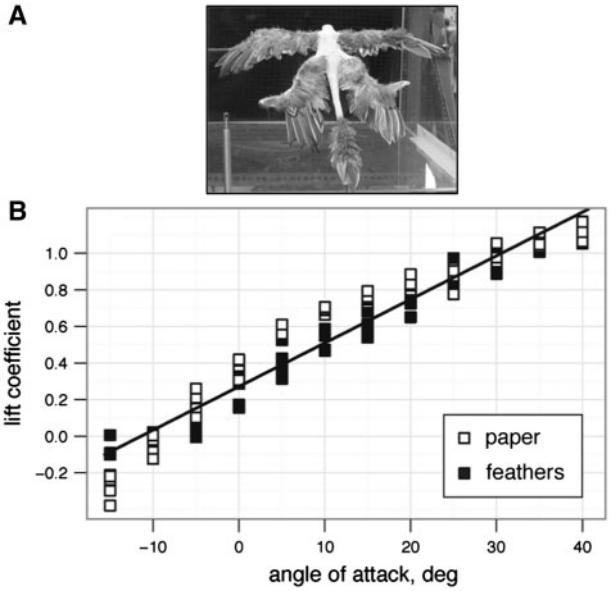

Fig. 5 (**A**) Photograph of a rear view of a model of †*M. gui* with real bird feathers. The model is in the sprawled posture and is mounted at an angle of attack of 30° in the wind tunnel. (**B**) Lift coefficient plotted as a function of angle of attack for models of †*M. gui* in the sprawled posture with paper feathers (open squares) and with bird feathers (black squares). Each symbol represents an independent replicate measurement. At each angle of attack, there was no significant difference between the lift coefficients of the model with feathers and the model with paper plumage (ANOVAs performed at each angle of attack, $P > 0.05$).

more guesswork is involved. We did not know the weights of †*M. gui*'s body parts, but we made the simplifying assumption that its tissue mass was uniform throughout its body, and then approximated its distribution of mass in our models by making them geometrically similar to the reconstructions of †*M. gui* (Fig. 1 of Xu et al. 2003)

The position of the COM of a model can be calculated or determined experimentally. If the coordinates of the body surface can be determined from 3D reconstructions of the organism or from drawings of its reconstructed frontal, sagittal, and transverse perimeters, then the body can be mathematically sliced into transverse sections. The position of the COM can be calculated from the masses, centroids, and moments of these slices, which are computed using assumed tissue densities (e.g., Henderson 1999). Alternatively, the fore-aft position of the center of mass of the model in a given posture can be found by hanging the model from a string attached at different positions along the centerline of the body or balancing the model on a knife edge held at right angles to the long axis of the body. Similarly, the right-left and up-down positions of the COM can be determined. We used both approaches for our models of †*M. gui* and got similar results. The pros and cons of different techniques for determining the COM are discussed by Hurlburt (1999).

The force transducer should be mounted within the model so that its center is located at the center of mass for the model. Mounting the sensor at locations other than the COM may be needed to avoid interference with wings or other body parts, to avoid creating wakes for downstream appendages, or to avoid saturation of force or torque sensors. When mounting at locations other than the COM is necessary, then the position of the transducer relative to the COM should be measured so that the forces and moments acting at the COM can be calculated from the transducer output.

Are the data reasonable?

If models are used to study extant organisms, then the performance of the model and the living organism can be compared, as described above (e.g., Emerson and Koehl 1990; Koehl 1977, 2003). However, when using models to study extinct organisms, the forces or performance indices measured for the models can be compared to their values for living organisms to see if they are similar. For example, the $(C_L/C_D)_{max}$ values that we measured for our models of †*M. gui* fall in the middle of the range of $(C_L/C_D)_{max}$'s for a variety of other gliding organisms (Fig. 6).

Conclusions and caveats

Dynamically scaled physical models are useful tools for investigating the effects of morphology and posture on the gliding performance of both living and extinct organisms. Measurements of lift, drag, side force, and moments in pitch, roll, and yaw on models in a wind tunnel can be used to calculate indices of gliding and parachuting performance, aerodynamic static stability, and control effectiveness in maneuvering. These indices permit the aerodynamic performance of bodies of different shapes, sizes, stiffnesses, textures, and postures to be compared, and thus can provide insights about the design of gliders, both biological and man-made. However, the diverse morphologies of gliding organisms make it difficult in many cases to use standard engineering conventions for some of the terms used in calculating performance indices. For example, the engineering conventions of using the wing chord length for L, or the planform area of the wings alone for S, are not workable for wingless animals. Similarly, the engineering convention of using the orientation of a wing relative to the airflow to

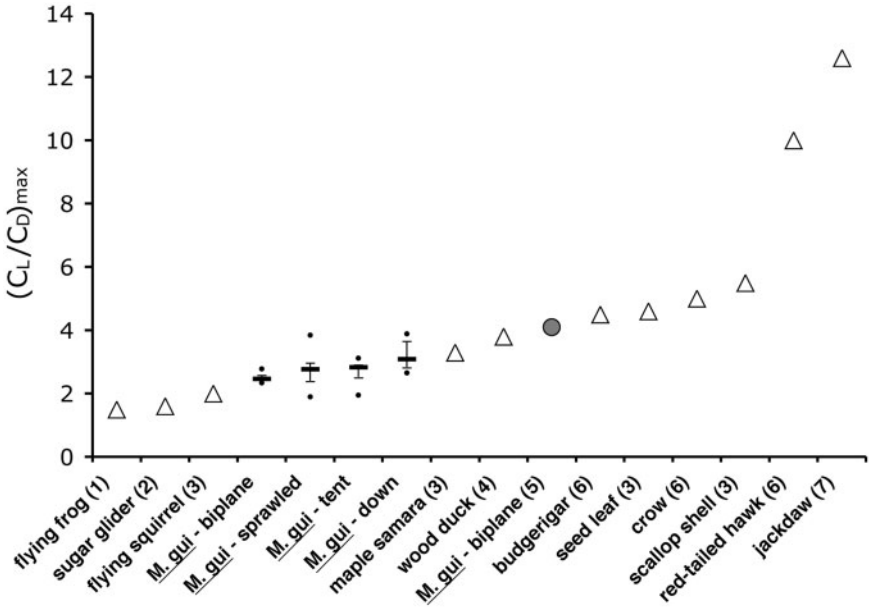

Fig. 6 Comparison of median values of $(C_L/C_D)_{max}$ for our models of †*M. gui* in various postures (error bars show quartiles, dots show range; five replicates per posture) with $(C_L/C_D)_{max}$ values for a variety of other gliding organisms (white triangles) published in the references indicated by the numbers in parentheses: (1) Emerson and Koehl (1990), (2) Bishop (2007), (3) Vogel (1994), (4) Withers (1981), (5) Tennekes (1996), and (6) Rosen and Hedenstrom (2001). Because both C_L and C_D are calculated using planform area [S in Equations (3) and (4)], S is canceled when $(C_L/C_D)_{max}$ is calculated, and therefore, the different definitions of S used for these diverse organisms does not affect $(C_L/C_D)_{max}$. There was no significant difference among the $(C_L/C_D)_{max}$'s of the postures of †*M. gui* that we tested (Kruskal–Wallis, $P > 0.05$). Our values for $(C_L/C_D)_{max}$ of †*M. gui* were slightly lower than those reported by Alexander et al. (2010) for freely-gliding models of †*M. gui* (gray circle).

determine the angle of attack (α) may not be appropriate for organisms with multiple body parts at different orientations. Therefore, care must be taken to define how L, S, and α are measured when reporting performance indices for organisms, and when comparing values from the literature.

Although studies using physical models to measure aerodynamic performance provide quantitative results, there are many sources of uncertainty when they are used to study the performance of extinct organisms. Body contours and mass distributions depend on the reconstructions done from fossilized skeletons and integumentary structures, the postures and behaviors that might have been used are inferred from those used by related living organisms and from constraints imposed by morphology (e.g., joints in the skeleton), the speeds they traveled through the air are estimated from speeds of living organisms of similar mass and wing loading, and the environmental conditions in which they operated (e.g., foliage and other obstructions in the habitat, organisms with which they might have interacted, air properties) may be inferred based on other fossils found nearby and the type and age of the rock formation in which the fossils were found. Furthermore, the aspects of aerodynamic performance that might have affected the fitness of the organisms must be guessed. Nonetheless, reasonable assumptions for model design can be made via careful study of the fossils, comparison of the species being studied with related extinct and extant species, and awareness that a single specimen or fragment might be misleading. If we keep these caveats in mind, then aerodynamic studies of extinct organisms let us test the feasibility of various hypotheses about their behavior, ecology, or evolution, and enable us to rule out those that are not physically feasible.

Our measurements of $(C_L/C_D)_{max}$ for physical models of †*M. gui* are similar to those measured by Alexander et al. (2010) for freely-gliding models of †*M. gui* (Fig. 6). Chatterjee and Templin (2007), who used mathematical modeling to compare the gliding performance of †*M. gui* with that of other gliding animals, concluded that †*M. gui* was a "moderate glider." We concur with that assessment after comparing our measurements of the $(C_L/C_D)_{max}$ of †*M. gui* with values measured for other gliding organisms (Fig. 6). Our measurements of $(C_L/C_D)_{max}$ of †*M. gui* also suggest that the various debated postures of the legs make little difference to horizontal distance traveled per vertical distance fallen during a glide. Although postures of the legs have little effect

on that aspect of gliding performance, we found that they do affect other aspects of aerodynamic performance, such as stability and maneuverability (to be reported in detail elsewhere). Similarly, measurements made in a wind tunnel by Davis et al. (2008, NOVA show cited above) suggested that †*M. gui* might have used the tent posture for gliding, but that the biplane posture could have been used to pitch the animal upwards so that it could land with its ventral surface on a tree trunk.

Both †*M. gui* and flying frogs have large aerodynamic surfaces on their hind limbs, posterior to the center of mass, but †*M. gui* also has large feathered forelimbs and a long feathered tail. The $(C_L/C_D)_{max}$ of †*M. gui* is about twice that of flying frogs (Emerson and Koehl 1990). We found that the aerodynamic pitching moment on †*M. gui* in the controversial sprawled posture is stable in pitch and thus, resists changes in pitch when the tail is moved up and down at most positive angles of attack (α, Fig. 3D). In contrast, in the range of α's around 0°, †*M. gui* in the sprawled posture is unstable in pitch and should be easier to maneuver than at higher α's. This example illustrates that orientation of the body relative to the flow past the animal determines whether or not a given posture is stable or unstable, and is difficult or easy to maneuver.

Acknowledgments

We thank the following URAP students for participating in this project: G. Cardona, C. Chun, M. Cohen, E. Guenther-Gleason, T. Hata, V. Howard, T. Huynh, S. Jaini, C. Kang, A. Kwong, F. Linn, C. Lopez, A. Lowenstein, D. Manohara, D. Marks, N. Ray A. Tisbe, K. Tse, F. Wong, O. Yu, F. and R. Zhu. We thank the Center for Integrative Biomechanics Education and Research (CIBER) for the use of their force transducer, and R. Dudley, H. Heatwole, Y. Munk, and two anonymous reviewers for advice that improved this article.

Funding

The Undergraduate Research Apprentice Program (URAP) at the University of California, Berkeley; National Science Foundation Minority Graduate Research Fellowship and Chancellor's Fellowship, University of California, Berkeley (to D.E.); National Science Foundation Integrative Graduate Education and Research Traineeship (IGERT) #DGE-0903711 (to R. Full, M.K., R. Dudley, and R. Fearing); the Virginia and Robert Gill Chair and MacArthur Fellowship (to M.K.).

References

Alexander McN. 1982. Locomotion in animals. New York: Chapman and Hall.

Alexander DE, Gong E, Martin LD, Burnham DA, Falk AR. 2010. Model tests of gliding with different hind wing configurations in the four-winged dromaeosaurid *Microraptor gui*. Proc Natl Acad Sci USA 107:2972–6.

Beebe CW. 1915. A tetrapteryx stage in the ancestry of birds. Zoologica 2:38–52.

Benson T. 2009. Air viscosity: Sutherland's formula [Internet]. National Aeronautics and Space Administration [accessed April 27, 2011]. Available from: http://www.grc.nasa.gov/WWW/BGH/viscosity.html.

Benton MJ, Zhonghe Z, Orr PJ, Fucheng Z, Kearns SL. 2008. The remarkable fossils from the Early Cretaceous Jehol Biota of China and how they have changed knowledge of Mesozoic life. Proc Geol Assoc 119:209–28.

Berner RA, Beerling DJ, Dudley R, Robinson JM, Wildman RA Jr. 2003. Phanerozoic atmopshereic oxygen. Ann Rev Earth Planet Sci 31:105–34.

Bishop K. 2007. Aerodynamic force generation, performance and control of body orientation during gliding in sugar gliders (*Petaurus breviceps*). J Exp Biol 210:2593–606.

Bock WJ. 1986. The arboreal origin of avian flight. Mem Cal Acad Sci 8:57–72.

Briggs DEG, Dalingwater JE, Selden PA. 1991. Biomechanics of locomotion in fossil arthropods. In: Rayner JMV, Wootton RJ, editors. Biomechanics in evolution. Cambridge: Cambridge University Press. p. 37–56.

Bundle MW, Dial KP. 2003. Mechanics of wing-assisted incline running (WAIR). J Exp Boil 206:4553–64.

Burgers P, Chiappe LM. 1999. The wing of *Archaeopteryx* as a primary thrust generator. Nature 399:60–2.

Chamberlain JA Jr. 1976. Flow patterns and drag coefficients of cephalopod shells. Paleontology 19:539–63.

Chamberlain JA Jr. 1981. Hydromechanical design of fossil cephalopods. In: House MR, Senior JR, editors. The Ammonoidea. London: Academic Press. p. 289–336.

Chatterjee S, Templin RJ. 2007. Biplane wing planform and flight performance of the feathered dinosaur *Microraptor gui*. Proc Nat Acad Sci USA 104:1576–80.

Christiansen P, Farina RA. 2004. Mass prediction in theropod dinosaurs. Hist Biol 16:85–92.

Dabiri JO, Colin SP, Costello JH. 2007. Morphological diversity of medusan lineages constrained by animal-fluid interactions. J Exp Biol 210:1868–73.

Dial KP. 2003. Wing-assisted incline running and the evolution of flight. Science 299:402–4.

Dial KP, Jackson BE, Segre P. 2008. A fundamental avian wingstroke provides a new perspective on the evolution of flight. Nature 451:985–9.

Dial KP, Randall RJ, Dial TR. 2006. What use is half a wing in the ecology and evolution of birds? Biosciences 56:437–45.

Dickinson MH, Lehmann FO, Sane SP. 1999. Wing rotation and the aerodynamic basis of insect flight. Science 284:1954–60.

Daniel TL. 1983. Mechanics and energetics of medusan jet propulsion. Can J Zool 61:1406–20.

Daniel TL, Helmuth BS, Saunders WB, Ward PD. 1997. Septal complexity in ammonoid cephalopods increased mechanical risk and limited depth. Paleobiology 23:470–81.
Dudley R. 1998. Atmospheric oxygen, giant Paleozoic insects and the evolution of aerial locomotor performance. J Exp Biol 201:1043–50.
Emerson SB, Koehl MAR. 1990. The interaction of behavior and morphology in the evolution of a novel locomotor type: ''Flying frogs.'' Evolution 44:1931–46.
Emerson SB, Travis J, Koehl MAR. 1990. Functional complexes and additivity in performance: a test case with flying frogs. Evolution 44:2153–7.
Etkin B, Reid LD. 1996. Dynamics of flight: stability and control. 3rd ed. New York: John Wiley and Sons.
Fucheng Z, Zhonghe Z, Duke G. 2006. Feathers and 'feather-like' integumentary structures in Liaoning birds and dinosaurs. Geol J 41:395–401.
Haynes WM, Lide DR, editors. 2011. CRC handbook of chemistry and physics. 91st ed. Boca Raton, FL: CRC Press.
Henderson DM. 1999. Estimating the mass and centers of mass of extinct animals by 3-D mathematical slicing. Paleobiology 25:88–106.
Hertel F, Campbell KE. 2007. The antitrochanter of birds: form and function in balance. Auk 124:789–805.
Heyer WR, Pongsapipatana S. 1970. Gliding speeds of *Ptychozoon lionatum* (Reptilia: Gekkonidae) and *Chrysopelea ornata* (Reptilia: Colubridae). Herpetologica 26:317–9.
Hoerner SF. 1965. Fluid-dynamic drag. Brick Town, NJ: Hoerner Fluid Dynamics.
Homberger DG. 2003. Avian origins revisited. J Biosci 28:135–8.
Hu D, Hou l, Zhang L, Xu X. 2009. A pre-*Archaeopteryx* trodontid theropod from China with long feathers on the metatarsus. Nature 461:640–3.
Hurlburt G. 1999. Comparison of body mass estimation techniques using recent reptiles and the pelycosaur *Edaphosaurus boanerges*. J Vert Paleo 19:338–50.
Hutchenson JR. 2003. Early birds surmount steep slopes. Nature 426:777–8.
Hutchenson JR. 2004. Biomechanical modeling and sensitivity analysis of bipedal running ability. I Extant taxa J Morphol 262:421–40.
Hutchenson JR, Allen V. 2009. The evolutionary continuum of limb function from early theropods to birds. Naturwissenschaften 906:423–48.
Kingsolver JG, Koehl MAR. 1985. Aerodynamics, thermoregulation, and the evolution of insect wings: differential scaling and evolutionary change. Evolution 39:488–504.
Kingsolver JG, Koehl MAR. 1994. Selective factors in the evolution of insect wings. Ann Rev Entomol 39:425–51.
Koehl MAR. 1977. Effects of sea anemones on the flow forces they encounter. J Exp Biol 69:87–105.
Koehl MAR. 1992. Hairy little legs: Feeding, smelling, and swimming at low Reynolds number. Fluid dynamics in biology. Contemp Math 141:33–64.
Koehl MAR. 1998. Small-scale hydrodynamics of feeding appendages of marine animals. Oceanography 11:10–2.
Koehl MAR. 2003. Physical modeling in biomechanics. Phil Trans Roy Soc B 358:1589–96.
Koehl MAR. 2004. Biomechanics of microscopic appendages: Functional shifts caused by changes in speed. J Biomech 37:789–95.
Kurochkin EN. 2006. Parallel evolution of theropod dinosaurs and birds. Ent Rev 86:545–58.
Long CA, Zhang GP, George TF, Long C. 2003. Physical theory, origin of flight, and a synthesis proposed for birds. J Theor Biol 224:9–26.
Longrich N. 2006. Structure and function of hindlimb feathers in *Archaeopteryx lithographica*. Paleobiology 32:417–31.
Maynard-Smith J. 1952. The importance of the nervous system in the evolution of animal flight. Evolution 6:127–9.
McCay MG. 2001. Aerodynamic stability and maneuverability of the gliding frog *Polypedates dennysi*. J Exp Biol 204:2817–26.
McCormick BW. 1995. Aerodynamics, aeronautics, and flight mechanics. 2nd ed. Hoboken, NJ: John Wiley and Sons.
Norberg RA. 1985. Flying, gliding, and soaring. In: Hildebrand M, Bramble D, Leim K, Wake D, editors. Functional vertebrate morphology. Cambridge: Belknap Press. p. 129–58.
Norberg UML, Brooke AP, Tiewhella WJ. 2000. Soaring and non-soaring bats of the family Pteropodidae (flying foxes *Pteropsus* spp.): wing morphology and flight performance. J Exp Biol 203:651–64.
Norell MA, Xu X. 2005. Feathered dinosaurs. Annu Rev Earth Pl Sc 33:277–99.
Nudds RL, Dyke G. 2009. Forelimb posture in dinosaurs and the evolution of the avian flapping flight-stroke. Evolution 63:994–1002.
Ostrom JH. 1986. The cursorial origin of avian flight. Mem Calif Acad Sci 8:73–81.
Padian K. 2003. Four-winged dinosaurs, bird precursors, or neither? Bio Sci 53:450–2.
Padian K, Chiappe LM. 1998. The origin and early evolution of birds. Biol Rev 75:1–42.
Padian K, Dial KP. 2005. Could 'four-winged' dinosaurs fly? Nature 438:E3.
Paul GS. 2003. Screaming biplane dromaesaurs of the air. Prehist Times 60:4–50.
Peczkis J. 1994. Implications of body-mass estimates for dinosaurs. J Vertebr Paleontol 14:520–33.
Pennycuick C. 1971. Gliding flight of the white-backed vulture *Gyps africanus*. J Exp Biol 55:13–38.
Pennycuick C. 1972. Animal flight. Institute of Biology Studies in Biology No. 33. Southampton: The Camelot Press.
Prum RO. 2003. Dinosaurs take to the air. Nature 421:323–4.
Rayner JMV, Wootton RJ, editors. 1991. Biomechanics in evolution. Cambridge: Cambridge University Press.
Reidenbach MA, George NT, Koehl MAR. 2008. Antennule morphology and flicking kinematics facilitate odor sampling by the spiny lobster, *Panulirus argus*. J Exp Biol 211:2849–58.
Rosen M, Hedenstrom A. 2001. Gliding flight in a jackdaw: a wind tunnel study. J Exp Boil 204:1153–66.
Ruben J. 2010. Paleobiology and the origins of avian flight. Proc Natl Acad Sci USA 107:2733–4.
Sellers WI, Manning PM. 2007. Estimating dinosaur maximum running speeds using evolutionary robotics. Proc Roy Soc Lond B 274:2711–6.

Senter P. 2006. Scapular orientation in theropods and basal birds, and the origin of flapping flight. Acta Palaentol Polonica 51:305–13.

Socha JJ, LaBarbera M. 2005. Effects of size and behavior on aerial performance of two species of flying snakes (Chrysopelea). J Exp Boil 208:1835–47.

Stanley SM. 1975. Why clams have the shape they have: An experimental analysis of burrowing. Paleobiology 1:48–58.

Tucker VA. 1990. Body drag, feather drag and interference drag of the mounting strut in a peregrine falcon, *Falco peregrinus*. J Exp Biol 149:449–68.

Tennekes H. 1996. The simple science of flight: from insects to jumbo jets. Cambridge, MA: MIT Press.

Usherwood JR, Ellington CP. 2002. The aerodynamics of revolving wings - I. Model hawkmoth wings. J Exp Biol 205:1547–64.

Vogel S. 1985. Flow-assisted shell reopening in swimming scallops. Biol Bull 169:624–30.

Vogel S. 1987. Flow-assisted mantle cavity refilling in jetting squid. Biol Bull 172:61–8.

Vogel S. 1994. Life in moving fluids. 2nd ed. Princeton, NJ: Princeton University Press.

Vogel S, Ellington CP, Kilgore DC Jr. 1973. Wind-induced ventilation of the burrow of the prairie dog, *Cynomys ludovicianus*. J Comp Physiol 85:1–14.

Withers PC. 1981. An aerodynamic analysis of bird wings as fixed aerofoils. J Exp Boil 0:143–62.

Witmer LM. 2009. Feathered dinosaurs in a tangle. Nature 462:601–2.

Xu X, Zhou ZH, Wang XL. 2000. The smallest known non-avian theropod dinosaur. Nature 408:705–8.

Xu X, Zhou Z, Wang X, Kuang X, Zhang F, Du X. 2003. Four-winged dinosaurs from China. Nature 421:335–40.

Xu X, Zhou Z, Wang X, Kuang X, Zhang F, Du X. 2005. Origin of flight: Xu et al. reply. Nature 438:E3–4.

Zhang FC, Zhou ZH. 2004. Leg feathers in an early Cretaceous bird. Nature 431:925.

Zhou Z. 2004. The origin and early evolution of birds: discoveries, disputes, and perspectives from fossil evidence. Naturwissenschaften 91:455–71.

Zhou Z. 2006. Evoltuionary radiation of the Jehol Biota: chronological and ecological perspectives. Geol J 41:377–93.

Zhou Z, Barrett PM, Hilton J. 2003. An exceptionally preserved lower Cretaceous ecosystem. Nature 421:807–14.

Zhou Z, Zhang FC. 2005. Origin of flight: could ''four-winged'' dinosaurs fly? Reply. Nature 438:E4.